

Production of Photo-oxidants by Dissolved Organic Matter During UV Water Treatment

Yaal Lester,[†] Charles M. Sharpless,[‡] Hadas Mamane,[§] and Karl G. Linden^{*,†}

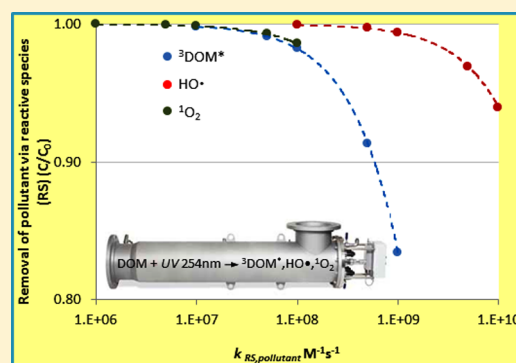
[†]Department of Civil, Environmental, and Architectural Engineering, University of Colorado, UCB 428, Boulder, Colorado 80309, United States

[‡]Department of Chemistry, University of Mary Washington, Fredericksburg, Virginia 22401, United States

[§]School of Mechanical Engineering, Faculty of Engineering, Tel Aviv University, Tel Aviv, 69978, Israel

S Supporting Information

ABSTRACT: Dissolved organic matter (DOM) irradiated by sunlight generates photo-oxidants that can accelerate organic contaminant degradation in surface waters. However, the significance of this process to contaminant removal during engineered UV water treatment has not been demonstrated, partly due to a lack of suitable methods in the deep UV range. This work expands methods previously established to detect ¹O₂, HO•, H₂O₂, and DOM triplet states (³DOM*) at solar wavelengths to irradiation at 254 nm, typical of UV water treatment. For transient intermediates, the methods include a photostable probe combined with selective scavengers. Quantum yields for ¹O₂, ³DOM* and H₂O₂ were in the same range as for solar-driven reactions but were an order of magnitude higher for HO•, which other experiments indicate is due to H₂O₂ reduction. With the quantum yields, the degradation of metoxuron was successfully predicted in a DOM solution irradiated at 254 nm. Further modeling showed that the contribution of DOM sensitization to organic contaminant removal during UV treatment should be significant only at high UV fluence, characteristic of advanced oxidation processes. Of the reactive species studied, ³DOM* is predicted to have the greatest general influence on UV degradation of contaminants.



INTRODUCTION

Ultraviolet irradiation (UV) is an established tool for the treatment of drinking and wastewater, effective for inactivating human pathogens¹ and for degrading various organic contaminants (e.g., pharmaceuticals).² UV is an attractive physical alternative to traditional chemical oxidants (i.e., chlorine and chloramine) that often produce disinfection byproducts.

A contaminant may be degraded by direct UV photolysis when it absorbs light and decomposes unimolecularly or reacts with dissolved oxygen. However, direct photolysis is only effective when the contaminant absorption spectrum overlaps the emission spectrum of the UV lamp and when the direct photolysis quantum yield is reasonably large. This is often not the case, and in these instances indirect photolysis is typically more important. Water constituents such as nitrate and dissolved organic matter (DOM) can act as photosensitizers to produce reactive species such as singlet oxygen (¹O₂) and hydroxyl radical (HO•). In the case of DOM sensitization, absorption of light leads to the formation of triplet excited states (³DOM*), themselves a potent oxidant for many aquatic contaminants³—that react with O₂ via energy or electron transfer mechanisms to generate reactive oxygen species such as ¹O₂, HO•, and H₂O₂.^{4–6}

DOM photochemistry at solar wavelengths ($\lambda > 300$ nm) has been investigated for several years,^{7–11} and the photo-oxidants are known to enhance organic contaminant transformation. For example, Gerecke et al.¹² attributed the photochemical elimination of numerous phenylurea herbicides from surface water to reaction with ³DOM*, while others have demonstrated the involvement of ¹O₂ and HO• in the elimination of different contaminants.¹³ With UV-C radiation (200–280 nm), commonly used in water treatment, the efficiency of photo-oxidant generation by DOM is presently unknown. This is primarily because available detection methods were developed for use with longer wavelengths, and many of the probe chemicals cannot be used (or require technical refinements) due to their direct degradation by UV-C radiation. As a result, the concentration of these species in deep UV systems and their contribution to UV degradation of water contaminants has not been previously evaluated.

The goals of this study were to validate methods for determining the quantum yields of photo-oxidants (•OH, ¹O₂, ³DOM*, and H₂O₂) generated by DOM under UV-C radiation

Received: June 28, 2013

Revised: September 5, 2013

Accepted: September 6, 2013

Published: September 6, 2013

and to assess their contribution to contaminant decay in engineered UV systems. The methods combine a selective, photostable probe compound with different scavengers and were applied to Suwannee River humic acid (SRHA) and fulvic acid (SRFA) as model DOM sensitizers. Using these results, the degradation of the phenylurea herbicide, metoxuron (MET), in an irradiated SRHA sample was successfully modeled, and the concentrations of the photo-oxidants were estimated in UV water treatment systems to assess their contribution to organic contaminant removal.

MATERIALS AND METHODS

Chemicals. Suwannee River humic acid (SRHA) and fulvic acid (SRFA) were obtained from the International Humic Substances Society (www.ihss.gatech.edu). Para-chlorobenzoic acid (pCBA), 2,4,6-trimethylphenol (TMP), *t*-butanol, hydrogen peroxide (H₂O₂), methanol, acetonitrile, sodium azide, 2,4-dinitrophenylhydrazine (DNPH), formaldehyde, and catalase were obtained from Sigma-Aldrich and were all at least analytical grade (>98%). Furfuryl alcohol (FFA) was from TCI America (Portland, OR) and metoxuron (MET) was from AccuStandards (New Haven, CT). Deionized water (resistance = 18.2 MΩ·cm) was obtained from a Millipore Milli-Q purification system. All chemicals were used as received except DNPH, which was recrystallized twice from acetonitrile.

Stock and Experimental Solutions. A stock solution of SRHA (500 mg/L) was prepared in Milli-Q water adjusted to pH 10 with NaOH. The stock of SRFA (500 mg/L) was prepared directly in Milli-Q water. Both stock solutions were filtered with a 0.45 μm cellulose acetate membrane and stored at 4 °C. Stock solutions of probe compounds were prepared in Milli-Q water. Experimental solutions were prepared in 5 mM phosphate buffered saline at pH 7.

Photochemical Experiments. UV exposures were performed using a quasi-collimated beam apparatus configured with four low-pressure mercury vapor lamps (ozone-free, General Electric No. G15T8) emitting predominantly at 253.7 nm. In a typical experiment, a 30 mL sample was irradiated with gentle stirring in a 50 × 35 mm crystallization dish (solution depth 2 cm) open to the atmosphere. Incident irradiance at the surface of the sample, measured by a calibrated radiometer (IL1700, SED 240/W, International Light, Peabody, MA), was 1.00 mW cm⁻² (2.12 × 10⁻⁶ millieinsteins s⁻¹ cm⁻²). Average irradiance was calculated using the appropriate correction factors (Bolton and Linden¹⁴), specifically: (i) divergence factor, accounting for the fact that the light beam is not fully collimated, (ii) reflection factor, for light reflection at the sample surface, and (iii) Petri factor, accounting for the nonuniformity of the radiation at the sample surface.

Analytical Methods. Molar absorption coefficients of the probes were measured using a Cary 100 Bio UV/vis spectrophotometer. Degradation of the compounds FFA, pCBA, TMP, and MET was followed by HPLC-UV (Agilent, model 1200, XDB C18 column 4.6 × 150 mm²) using isocratic elution with water (at pH 3) containing varying percentages of methanol. Dissolved organic carbon (DOC) was measured using a TOC-VSCH analyzer (Shimadzu Corp., Japan). Total iron in the SRHA and SRFA solutions was determined using HACH method 8008. The concentration of H₂O₂ was determined by the molybdate-activated iodide method. This method utilizes a color change that occurs when H₂O₂ reacts with KI in a buffered solution containing ammonium

molybdate, forming I₃⁻ which can be detected spectrophotometrically at 352 nm.¹⁵

RESULTS AND DISCUSSION

Detection Methods and Probes. An ideal probe compound should be selective toward the target reactive species and not decay under UV-C exposure. Therefore, our approach included testing the photostability of selected probes and testing the selectivity of the probes for the target photo-oxidants using different scavengers. Experiments were carried out at least in duplicate using either Milli-Q water (for direct photolysis) or SRHA solution (at 15 mgC L⁻¹) at pH 7.

Singlet Oxygen (¹O₂). Generation of ¹O₂ at wavelengths >300 nm is commonly probed by FFA, which reacts selectively with ¹O₂ ($k_{\text{FFA},^1\text{O}_2} = 1.2 \times 10^8 \text{ M}^{-1} \text{ s}^{-1}$).⁸ Direct photolysis of FFA at 254 nm ($C_0 = 25 \text{ μM}$) was found to be very slow (results not shown), due to the probe's low molar absorption coefficient ($\epsilon_{254} = 19.5 \pm 0.97 \text{ M}^{-1} \text{ cm}^{-1}$; Table 1) and quantum yield (Φ_p). The direct photolysis quantum yield was calculated as 0.032 ± 0.003 (Table 1) from the linear regression of FFA first-order decay kinetics.¹⁶

$$-\ln \frac{[\text{FFA}]_t}{[\text{FFA}]_0} = \frac{E_p^0 \epsilon (1 - 10^{-az})}{az} \Phi_p t = k' t \quad (1)$$

Here, $[\text{FFA}]_0$ and $[\text{FFA}]_t$ are the concentrations of FFA initially and at time t (s), respectively. E_p^0 is the incident photon irradiance (millieinstein cm⁻² s⁻¹), corrected for nonhomogeneity, ϵ is the FFA molar absorption coefficient (M⁻¹ cm⁻¹), a is the sample absorption coefficient (cm⁻¹), z is the depth of solution (cm), and k' is the first-order degradation rate constant of FFA (s⁻¹).

Degradation of FFA was further examined in SRHA solution with different scavengers, specifically: (i) no added scavenger, (ii) 50 mM *t*-butanol, and (iii) 50 mM *t*-butanol and 1 mM sodium azide (NaN₃). The concentration of *t*-butanol was selected to scavenge all available HO•, based on preliminary experiments. In these experiments, increasing concentrations of *t*-butanol were added to an irradiated solution of FFA and SRHA. The degradation rate of FFA decreased with increasing *t*-butanol concentration up to 25 mM. Further increasing *t*-butanol to 50 mM did not result in additional inhibition. Azide reacts with both HO• ($k_{\text{HO}\cdot, \text{N}_3} = 1.2 \times 10^{10} \text{ M}^{-1} \text{ s}^{-1}$)¹⁷ and ¹O₂ ($k_{^1\text{O}_2, \text{N}_3} = 5 \times 10^8 \text{ M}^{-1} \text{ s}^{-1}$).¹⁸ Therefore, its use to selectively scavenge ¹O₂ is most effective in the presence of *t*-butanol, which eliminates the influence of HO•. The FFA direct photolysis rate in the SRHA solution was calculated via eq 1, accounting for light attenuation by DOM.

In all cases, FFA decay exhibited pseudo-first order kinetics (Figure 1). As expected, direct photolysis was negligible. Adding *t*-butanol to the solution decreased the degradation rate of FFA by approximately 50%, indicating an important role of DOM sensitized HO• in FFA degradation at 254 nm. These results differ from what is typically observed in sunlight where degradation of FFA by HO• is negligible (<5%).¹⁹ Apparently, HO• formation increases under UV-C irradiation, resulting in a lower $[\text{O}_2]_{\text{ss}}/[\text{HO}\cdot]_{\text{ss}}$ steady-state concentration ratio relative to solar wavelengths.

Adding 1 mM NaN₃ in addition to *t*-butanol suppressed FFA degradation to approximately 40% of its rate with *t*-butanol alone. This can be adequately explained by assuming that azide is quenching photogenerated ¹O₂. The main (natural) decay

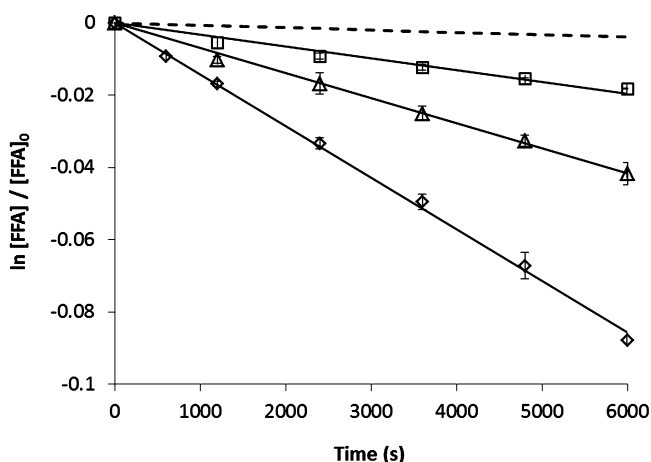


Figure 1. Degradation of FFA in a 254 nm irradiated SRHA solution (15 mgC L^{-1}): (\diamond) no added scavengers, (Δ) with 50 mM *t*-butanol, (\square) with 50 mM *t*-butanol and 1 mM NaN_3 , and (---) calculated direct photolysis.

path for $^1\text{O}_2$ is quenching by water ($k_d = 2.5 \times 10^5 \text{ s}^{-1}$).⁹ Therefore, adding 1 mM NaN_3 to the solution should reduce the $^1\text{O}_2$ concentration to approximately 33% of its concentration without NaN_3 . The measured decrease to 40% agrees well with that prediction. These results indicate that, in the presence of 50 mM *t*-butanol, reaction with $^1\text{O}_2$ is most likely the main path for FFA elimination, and that this method can be used to probe the generation of $^1\text{O}_2$ by DOM with UV-C radiation. It should be noted however, that although the results we obtained with azide are strong evidence that FFA is selective for $^1\text{O}_2$ in SRHA solution, $^3\text{DOM}^*$ may interfere with $^1\text{O}_2$ measurements by directly reacting with FFA, as previously demonstrated for aqueous anthraquinone-2-sulfonate and a whole water sample from Canal Fumemorte, France.^{20,21}

Degradation of FFA by $\text{HO}\bullet$ or $^1\text{O}_2$, calculated by subtracting other degradation pathways (Figure 1), was used to evaluate the photo-oxidants' steady state concentration in the irradiated SRHA sample (for calculation details, see Supporting Information, SI). Concentrations of $^1\text{O}_2$ and $\text{HO}\bullet$ were $5.3 \times 10^{-14} \text{ M}$ ($^1\text{O}_2$) and $9.9 \times 10^{-16} \text{ M}$ ($\text{HO}\bullet$), making the ratio $[\text{O}_2]_{\text{ss}}/[\text{HO}\bullet]_{\text{ss}}$ equal to 58. This is more than 2-fold lower than typical ratios measured above 300 nm (>100),²² emphasizing the increased importance of $\text{HO}\bullet$ relative to $^1\text{O}_2$ under UV-C radiation.

Hydroxyl Radical ($\text{HO}\bullet$). Two methods were tested to detect $\text{HO}\bullet$: (i) degradation of the probe compound pCBA, and (ii) α -H atom abstraction of methanol by $\text{HO}\bullet$ and monitoring the formation rate of the main stable product,

formaldehyde ($\text{HO}\bullet + \text{CH}_3\text{OH} \rightarrow \text{HCHO}$; $\Phi = 0.93$ ²³). pCBA and methanol were chosen as probes because they react with $\text{HO}\bullet$ via completely different mechanisms, their reaction rate constants with $\text{HO}\bullet$ are well-known, their direct photolysis is relatively slow, and their reactions can be followed by HPLC with fairly high sensitivity.^{11,24} As shown below and in the SI, the two methods provide comparable results. Other methods were evaluated, including the reaction of terephthalate and benzene with $\text{HO}\bullet$ and the monitoring the hydroxylation products. These methods were deemed unsuitable due to the photoinstability of hydroxyterephthalate²⁵ and benzene (this study, results not shown) under UV-C radiation.

Direct photolysis of pCBA ($C_0 = 1 \mu\text{M}$), measured in Milli-Q water, was slow but significant in relation to sensitized photolysis (Figure 2), with ϵ_{254} and quantum yield (Φ_p) of

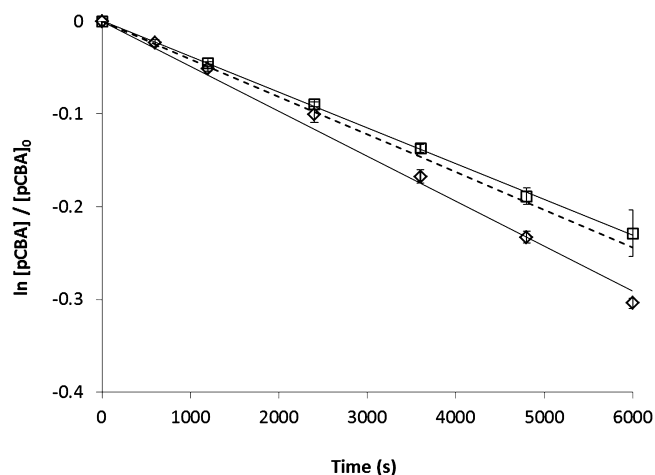


Figure 2. Degradation of pCBA in a 254 nm irradiated SRHA solution (15 mgC L^{-1}): (Δ) no added scavengers, (\square) with 50 mM *t*-butanol, and (---) calculated direct photolysis.

$2050 \pm 10 \text{ M}^{-1} \text{ cm}^{-1}$ and 0.016 ± 0.001 , respectively (Table 1). Degradation of pCBA in the presence of SRHA was tested with and without 50 mM *t*-butanol (Figure 2). Addition of *t*-butanol decreased the pCBA degradation to near its calculated direct photolysis rate. This implies that $\text{HO}\bullet$ is the main species responsible for sensitized pCBA degradation. Thus, by subtracting direct photolysis, pCBA can be used to probe $\text{HO}\bullet$ with UV-C radiation. To validate the pCBA method, we calculated the steady-state concentration of $\text{HO}\bullet$ and compared it to the value obtained using FFA. The $\text{HO}\bullet$ concentration were $1.6 \times 10^{-15} \text{ M}$ and $9.9 \times 10^{-16} \text{ M}$, using pCBA and FFA, respectively. These values are in excellent agreement considering the different initial concentrations of the

Table 1. Molar Absorption Coefficients (ϵ), Direct Photolysis Quantum Yields (Φ_p), and First-Order Decay Rate Constants for the Probes with SRHA (15 mgC L^{-1} , pH 7)

	pCBA	FFA	TMP
$\epsilon \text{ (M}^{-1}\text{cm}^{-1}\text{)}$	2045 (± 10)	19.5 (± 0.97)	321 (± 2)
Φ_p	0.016 (± 0.001)	0.032 (± 0.003)	0.05 (± 0.02)
first-order rate constant (k' , s^{-1})			
direct photolysis	4.07×10^{-5}	0.65×10^{-6}	1.46×10^{-5}
w/o scavengers	$5.06 (\pm 0.08) \times 10^{-5}$	$14 (\pm 1) \times 10^{-6}$	$1.4 (\pm 0.2) \times 10^{-4}$
with <i>t</i> -butanol	$3.9 (\pm 0.4) \times 10^{-5}$	$7.0 (\pm 0.4) \times 10^{-6}$	$1.5 (\pm 0.2) \times 10^{-4}$
with <i>t</i> -butanol and NaN_3^-		$3.0 (\pm 0.1) \times 10^{-6}$	
with FFA			$1.30 (\pm 0.09) \times 10^{-4}$

probes, i.e., 25 μM FFA and 1 μM pCBA. At these concentrations, pCBA will have negligible effect on $\text{HO}\bullet$ concentration, while FFA is expected to reduce the $\text{HO}\bullet$ concentration by $\sim 40\%$ (compared to a sample without probes).

In the methanol/formaldehyde method, a SRHA solution was irradiated in the presence of 0.4 M methanol. Under these conditions, more than 99% of photogenerated $\text{HO}\bullet$ reacts with methanol to generate formaldehyde as the main stable product ($k_{\text{methanol},\text{HO}\bullet} = 9.7 \times 10^8 \text{ M}^{-1} \text{ s}^{-1}$).²⁶ Detection of formaldehyde was carried out by HPLC-UV after reaction with 2,4-dinitrophenylhydrazine to form the hydrazone derivative, which absorbs at 370 nm.¹¹ A linear buildup of formaldehyde was recorded with time (Figure 3), indicating a detectable $[\text{HO}\bullet]_{\text{ss}}$.

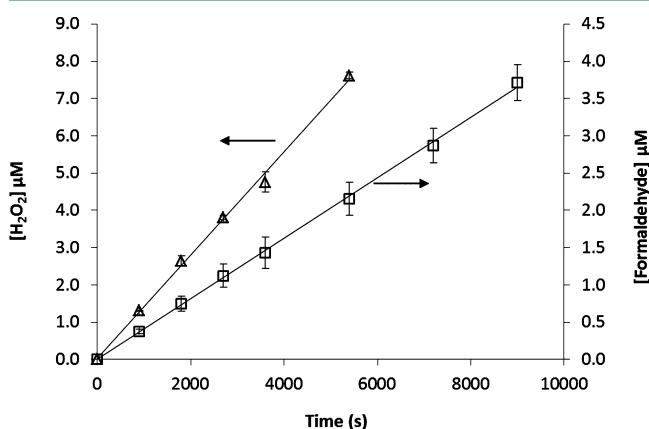


Figure 3. Concentration of (□) formaldehyde and (Δ) H_2O_2 as a function of time in a 254 nm irradiated solution of SRHA (15 mgC L^{-1} , pH 7). Experiments for formaldehyde conducted with 0.4 M methanol.

Hydrogen Peroxide (H_2O_2). When determining H_2O_2 by the molybdate/iodide method, the absorbance of the reagent-sample mixture was typically time dependent, and reached a maximum at approximately 1 min from mixing the sample and reagents, after which it slowly drifted downward, presumably due to reaction of I_3^- with DOM. Similar to other researchers, we took the maximum absorbance as the analytical signal.⁴

The H_2O_2 concentration increased linearly with time (Figure 3). To ensure that the method was selectively detecting H_2O_2 and not other long-lived oxidants produced at 254 nm, SRHA was irradiated for 25 min and tested for: (i) H_2O_2 concentration, (ii) H_2O_2 concentration after sample exposure to 20 units/mL catalase for 10 min, and (iii) H_2O_2 concentration after the addition of 2 μM H_2O_2 . Results showed the presence of 2.4 μM H_2O_2 in the first test, 0 μM H_2O_2 in the second, and 4.3 μM H_2O_2 in the third, indicating that the method is indeed selective and accurate for H_2O_2 .

Excited Triplet State of DOM ($^3\text{DOM}^*$). To detect $^3\text{DOM}^*$ we utilized 2,4,6-trimethylphenol (TMP), which is commonly used above 300 nm ($k_{\text{TMP},^3\text{DOM}^*} > 1 \times 10^9 \text{ M}^{-1} \text{ s}^{-1}$).^{20,27} Direct UV-C photolysis of TMP was found to be slow, with ϵ_{254} and Φ_p of $321 \pm 2 \text{ M}^{-1} \text{ cm}^{-1}$ and 0.05 ± 0.02 , respectively (Table 1). Degradation of TMP with SRHA was examined under the following conditions: (i) with no added scavenger, (ii) with 50 mM *t*-butanol, (iii) with 1 mM FFA, and (iv) after sparging with either O_2 or N_2 . Irradiation of the sparged samples (including a “non-sparged” blank) was conducted in sealed 1 cm quartz cuvettes placed at a 45° angle under the lamp.

TMP was readily degraded in the presence of UV irradiated SRHA with no added scavenger (Figure 4). Adding either 50

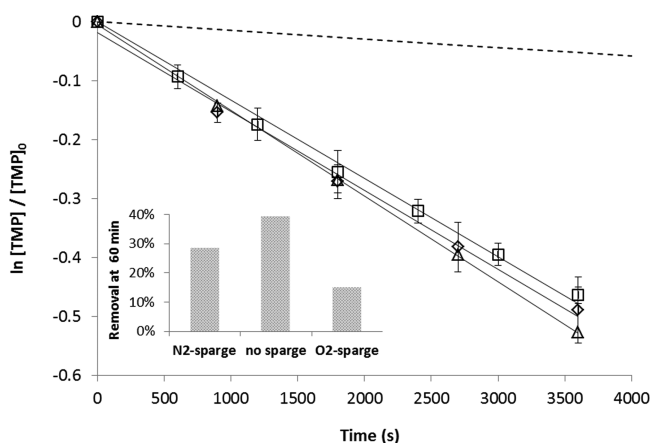


Figure 4. Degradation of TMP in a 254 nm irradiated SRHA solution (15 mgC L^{-1} , pH 7): (◇) no added scavengers, (Δ) with 50 mM *t*-butanol, (□) with 1 mM FFA, and (---) calculated direct photolysis. Inset: influence of N_2 and O_2 sparging on % removal of TMP after 60 min irradiation.

mM *t*-butanol or 1 mM FFA marginally affected the degradation, suggesting that reactions with $\text{HO}\bullet$ and $^1\text{O}_2$ are insignificant. At 1 mM, FFA reduces the concentration of $^1\text{O}_2$ by approximately 33%, which would suppress the degradation of TMP if reaction with $^1\text{O}_2$ was involved, but no effect was observed. Furthermore, $^1\text{O}_2$ reacts with TMP at a rate of $k_{\text{TMP},^1\text{O}_2} = 6.2 \times 10^7 \text{ M}^{-1} \text{ s}^{-1}$;²⁸ therefore, at $5.26 \times 10^{-14} \text{ M}$, $^1\text{O}_2$ should be responsible for less than 3% of the TMP degradation. We also examined the possibility of quenching $^3\text{DOM}^*$ with sorbic acid as a mechanistic test, but at suitable concentrations to act as a quencher it absorbed far too much light at 254 nm to be useful.

Sparging the solution with either O_2 or N_2 decreased the degradation rate of TMP relative to the non-sparged sample (inset, Figure 4). A similar trend was observed by Golanoski et al.,²⁹ where photodegradation of TMP in the presence of DOM (under simulated solar light) was highest at approximately 50 μM O_2 . This behavior was modeled by assuming that TMP reacts with $^3\text{DOM}^*$ to generate $\bullet\text{TMP}^+$ (and DOM^\bullet), immediately deprotonating to the phenoxyl radical, which requires O_2 to react further.²⁹ Alternatively, Maurino et al.³⁰ have proposed that O_2 is required for further reaction with DOM^\bullet instead. In both cases, the decreased TMP decay rate at low O_2 concentration is due to reformation of TMP upon reduction of the phenoxyl radical by the organic matter.^{29,30} The decreased TMP degradation rate at high O_2 concentration can be explained by O_2 quenching of $^3\text{DOM}^*$ ²⁹ and/or the reaction of DOM with O_2 to generate O_2^- , which may further reduce the phenoxyl radical back to TMP.³⁰

The above results indicate that TMP degradation under UV-C radiation occurs almost exclusively via reaction with $^3\text{DOM}^*$, making it a valid probe in this wavelength region.

Photo-oxidant Quantum Yields. The quantum yields of the photo-oxidants were determined for both SRFA and SRHA at 15 mgC L^{-1} and pH 7. The results are summarized in Table 2 with comparable values from the literature, and the calculations are detailed in the SI.

Table 2. Quantum Yields of the Photo-oxidants^a

	HO•		¹ O ₂		H ₂ O ₂		³ DOM* ^b	
	SRHA	SRFA	SRHA	SRFA	SRHA	SRFA	SRHA	SRFA
253.7 nm	0.048 (±0.004)	0.047 (±0.006)	1.4 (±0.08)	3.2 (±0.05)	0.139 (±0.005)	0.110 (±0.003)	120 (±20)	120 (±20)
>300 nm	0.003 ^c	0.004 ^c	1.59 ^e	2.11 ^e	0.04–0.06 ^g	0.06–0.08 ^g	36–76 ^h	14–59 ^h
		0.003–0.009 ^d	0.59–4.5 ^f		0.011–0.053 ^f			34 ⁱ

^aValues expressed as % except for ³DOM* (see notes). ^bQuantum yield coefficient (*f*, M⁻¹). ^cSolar light, Fluka humic acid.³⁷ ^d300 to 360 nm.⁵ ^eSimulated solar light.⁴² ^f300 to 400 nm, different DOM isolates.⁴ ^g300 to 360 nm.⁶ ^h313 and 336 nm.²⁷ ⁱ366 nm.¹²

The ¹O₂, ³DOM*, and H₂O₂ quantum yields were in the same range as for solar-driven reactions, although the ¹O₂ quantum yield for SRFA was approximately two-fold greater than that reported above 300 nm.¹⁰ In the case of HO•, however, the quantum yields were a full order of magnitude higher (Table 2). These trends may be explained by the different mechanisms and chromophores responsible for the generation of the different species. Oxidizing triplets (³DOM*), and consequently ¹O₂, are believed to arise from electron-acceptor type chromophores such as aromatic ketones²⁷ and quinones.²⁹ These chromophores absorb light over a wide spectral range in both the visible and deep UV. H₂O₂, on the other hand, is thought to be formed through sensitization of electron-donor type chromophores (e.g., substituted phenols), resulting in electron transfer to dissolved O₂ to form O₂⁻ and subsequently H₂O₂.⁶ Phenol moieties principally absorb in the UV-C range, so a significant increase in H₂O₂ yield should be expected at 254 nm. The moderate increase observed in our study likely results from reduction of H₂O₂ by photosensitized hydrated electrons to generate HO•, as explained below.

Several pathways have been proposed for generation of HO• by irradiated DOM, including hydrogen abstraction from water by quinone triplets³¹ and H₂O₂-dependent paths.³² To determine if H₂O₂ was contributing significantly to HO• production in the UV-C, experiments were conducted with pCBA and SRHA in the presence of 10 units/mL catalase (~0.02 μM, contributing no detectable absorbance) to quickly quench any H₂O₂ generated. The degradation rate of pCBA decreased significantly in the presence of catalase and was similar to its calculated direct photolysis, indicating that in the UV-C range HO• is mostly produced through H₂O₂. Direct HO• scavenging by catalase was negligible, assuming a conservative rate constant for the reaction of catalase with HO• of 10¹⁰ M⁻¹ s⁻¹ (10¹⁰ M⁻¹ s⁻¹ × 0.02 × 10⁻⁶ M = 200 s⁻¹). Different mechanisms are plausible for HO• formation via H₂O₂, including Fenton reactions,⁵ direct photolysis of H₂O₂³³ and reduction of H₂O₂ by DOM-sensitized hydrated electrons.³⁴ Direct photolysis of H₂O₂ in the SRHA solution was calculated to produce less than 20% of the HO•. The iron content of the SRHA/SRFA solutions was below the detection limit of the method (<0.36 μM Fe), which suggests a minor role for dark-Fenton reactions in the HO• production. Therefore, we hypothesize that in the UV-C range HO• is mainly produced through the reduction of H₂O₂ by DOM-sensitized hydrated electrons or possibly photo-Fenton reactions which require a small amount of iron.

Degradation of a Model Contaminant. Degradation of MET, a phenylurea herbicide, was measured and modeled using the validated methods and calculated quantum yields. Metoxuron (MET) was selected as a model contaminant due to its environmental relevance and its fast reaction with ³DOM*.¹² Photodegradation of MET in the presence of DOM

can be described as the sum of its direct photolysis and reactions with ¹O₂, HO• and ³DOM*:

$$k'_{\text{tot}} = k'_{\text{UV}} + k_{\text{O}_2}[\text{}^1\text{O}_2]_{\text{ss}} + k_{\text{HO}\bullet}[\text{HO}\bullet]_{\text{ss}} + k_{\text{DOM}^*}[\text{}^3\text{DOM}^*]_{\text{ss}} \quad (2)$$

where, *k'*_{tot} and *k'*_{UV} are the total and direct photolysis first-order rate constants, respectively. The other rate constants are for the second-order reactions of MET with ¹O₂, HO•, and ³DOM*. Reaction of MET with H₂O₂ was determined to be insignificant because 10 mg L⁻¹ H₂O₂ produced no loss of MET after dark reaction for 24 h in separate tests. The degradation rate of MET was calculated and measured for 15 mgC L⁻¹ SRHA and an irradiance of 1 mW cm⁻². All kinetic parameters for eq 2 are summarized in Table 3, and the calculations are detailed in the SI.

The calculated rate for MET degradation (2.9 × 10⁻⁴ s⁻¹) was in excellent agreement with the measured value of 3.0 ± 0.3 × 10⁻⁴ s⁻¹, indicating that the model accurately accounts for the majority of important parameters. Under our conditions, direct photolysis, HO• and ³DOM* contribute to MET degradation 76%, 3%, and 21%, respectively. The relatively high contribution of ³DOM* can be attributed both to its high steady-state concentration and its fast reaction with MET. Although this is one of the fastest reactions with ³DOM*, it may nevertheless be representative of a wide range of environmentally relevant contaminants such as phenols, sulfa, and amine drugs, which also react readily with ³DOM*.^{12,13,27,35}

Implications for UV Water Treatment. To assess the contribution of DOM sensitization in field-scale UV treatment, we considered a typical annular UV reactor of 8 × 80 cm (internal) dimensions, with a center-mounted 100 W LP UV lamp. The rate of light absorption by DOM was calculated as 1.6 × 10⁻⁵ einsteins L⁻¹ s⁻¹ using the following equation:

$$R_a = \frac{PE_f}{U} [1 - 10^{-az}] / V \quad (3)$$

where, *P* is the lamp power (W), *E_f* is the lamp's efficiency in the UV-C range (taken as 0.35),³⁶ *U* is the molar photon energy at 254 nm (J einsteins⁻¹), *z* is the light path (cm), and *V* is the reactor's volume (L). The water absorption coefficient (*a*) was set at 0.155 cm⁻¹ (equivalent to UV transmittance of 70%), typical for wastewater effluent. The photoreactivity of SRHA and SRFA is not substantially different from that of effluent organic matter;³⁷ therefore, their quantum yields can be used to predict the photo-oxidant formation rates in wastewater effluent.

Concentrations of ¹O₂, HO•, and ³DOM* were calculated to be 1.5 × 10⁻¹², 6.7 × 10⁻¹⁴, and 2.0 × 10⁻¹² M, respectively, using the steady-state assumption and quantum yields from Table 2. For HO•, scavenging by water constituents was

Table 3. Calculated Kinetic Parameters for the Photo-Degradation of MET with SRHA

	photolysis	$^1\text{O}_2$	$\text{HO}\bullet$	$^3\text{DOM}^*$	total
k_{RS} ($\text{M}^{-1} \text{s}^{-1}$)			5.8×10^9	1.0×10^9	
$[\text{RS}]_{\text{ss}}$ (M) ^a		5.3×10^{-14}	1.6×10^{-15}	6.1×10^{-14}	
k' (s^{-1})	2.2×10^{-4}		9.1×10^{-6}	6.1×10^{-5}	2.9×10^{-4}
contribution	76%		3%	21%	100%

^aRS, reactive species.

calculated assuming DOM and bicarbonate concentrations of 5 mgC L^{-1} and 3 mM, respectively. The contribution of H_2O_2 to the degradation process was considered negligible.

Figure 5 presents the predicted removal of hypothetical organic contaminants by $^1\text{O}_2$, $\text{HO}\bullet$, and $^3\text{DOM}^*$ as a function

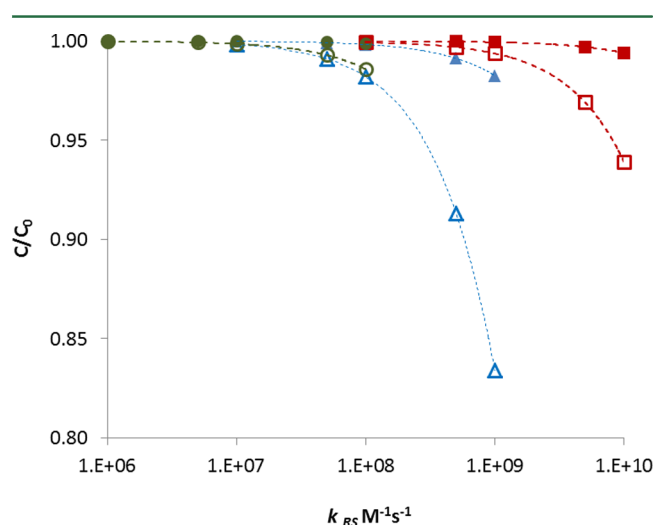


Figure 5. Expected removal of hypothetical organic contaminants during UV water treatment by photogenerated (Δ) $^3\text{DOM}^*$, (\square) $\text{HO}\bullet$, and (\circ) $^1\text{O}_2$, as a function of the contaminants' rate constants for reaction with the different species. Filled and unfilled symbols correspond to UV doses at 254 nm of 100 mJ cm^{-2} and 1000 mJ cm^{-2} , respectively.

of the contaminants' rate constant for reaction with the different reactive species (k_{RS}) at two different UV doses. The selected ranges of k_{RS} were 10^6 to $10^8 \text{ M}^{-1} \text{ s}^{-1}$ ($^1\text{O}_2$),³⁸ 10^8 to $10^{10} \text{ M}^{-1} \text{ s}^{-1}$ ($\text{HO}\bullet$)³⁹ and 10^7 to $10^9 \text{ M}^{-1} \text{ s}^{-1}$ ($^3\text{DOM}^*$).³ The selected UV doses (H , mJ cm^{-2}) were 100 and 1000 mJ cm^{-2} , representative of microbial disinfection and advanced oxidation (UV/ H_2O_2) applications, respectively. The UV dose was used to calculate the contaminant's residence time inside the reactor (RT):

$$\text{RT} = \frac{H}{E_{\text{avg}}} \quad (4)$$

$$E_{\text{avg}} = PE_f \left[\frac{1 - 10^{-az}}{2.3az} \right] / S \quad (5)$$

where, E_{avg} is the average fluence rate inside the reactor (mW cm^{-2}), and S is the surface area of the reactor (cm^2).

At disinfection doses (e.g., 100 mJ cm^{-2}) DOM-sensitized removal of contaminants is less than 3%. However, the contribution of DOM sensitization to UV degradation of water contaminants becomes significant at high UV doses, with up to 24% removal at 1000 mJ cm^{-2} (by $^3\text{DOM}^*$, $\text{HO}\bullet$, and $^1\text{O}_2$ combined). Triplet states are the principal contributors (up

to 17% removal), implying that mainly contaminants that react quickly with $^3\text{DOM}^*$ will be susceptible to sensitized degradation.

The predicted contribution of DOM to UV degradation of certain contaminants is comparable to what has been found for nitrate, a known $\text{HO}\bullet$ sensitizer. Keen et al.⁴⁰ showed that disinfection doses of polychromatic UV irradiation of wastewater containing nitrate may result in up to 30% removal of organic contaminants by sensitized $\text{HO}\bullet$. Higher doses of 2000 mJ cm^{-2} could lead to at least 20 to 70% sensitized oxidation for most contaminants. Similarly, Sharpless et al.⁴¹ showed that approximately 50% of the degradation of atrazine in UV water treatment could be attributed to reaction with $\text{HO}\bullet$ produced at typical concentrations of nitrate. In the case of DOM sensitization, applying 2000 mJ cm^{-2} may increase the removal of $^3\text{DOM}^*$ reactive contaminants by up to 40%.

The additive contribution of these two sensitizers, DOM and nitrate, may present a significant degradation pathway for different contaminants in wastewater, especially at UV doses used in advanced oxidation systems. This suggests the potential for using elevated UV doses to effect direct treatment of pharmaceuticals and other emerging contaminants in wastewater.³⁹ The results presented here also provide a tool for more accurate modeling of DOM's influence on UV water treatment beyond its generally accepted role as an $\text{HO}\bullet$ scavenger. Proper assessment of the rates of sensitized reactions may also allow better optimization of H_2O_2 doses in advanced oxidation (i.e., UV/ H_2O_2), a major operational cost in these systems. In this regard, it will be desirable to establish a better understanding of DOM's role in reducing H_2O_2 to $\text{HO}\bullet$ when UV-C radiation is used.

■ ASSOCIATED CONTENT

📄 Supporting Information

Spectrum of low-pressure Hg lamp, calculation of $^1\text{O}_2$ and $\text{HO}\bullet$ concentrations using FFA, calculation methods of the photo-oxidants' quantum yields and calculation of kinetics parameters for MET photodegradation. This material is available free of charge via the Internet at <http://pubs.acs.org>.

■ AUTHOR INFORMATION

✉ Corresponding Author

*Phone: 303-492-4798; fax: 303-492-7317; e-mail: karl.linden@colorado.edu.

📝 Notes

The authors declare no competing financial interest.

■ ACKNOWLEDGMENTS

This research was supported in part by the Water Environment Research Foundation (Grant U2R11).

■ REFERENCES

- (1) Hijnen, W. A. M.; Beerendonk, E. F.; Medema, G. J. Inactivation credit of UV radiation for viruses, bacteria and protozoan (oo)cysts in water: A review. *Water Res.* **2006**, *40*, 3–22.
- (2) Canonica, S.; Meunier, L.; von Gunten, U. Phototransformation of selected pharmaceuticals during UV treatment of drinking water. *Water Res.* **2008**, *42*, 121–128.
- (3) Canonica, S.; Hellrung, B.; Muller, P.; Wirz, J. Aqueous oxidation of phenylurea herbicides by triplet aromatic ketones. *Environ. Sci. Technol.* **2006**, *40*, 6636–6641.
- (4) Dalrymple, R. M.; Carfagno, A. K.; Sharpless, C. M. Correlations between dissolved organic matter optical properties and quantum yields of singlet oxygen and hydrogen peroxide. *Environ. Sci. Technol.* **2010**, *44*, 5824–5829.
- (5) Vaughan, P. P.; Blough, N. V. Photochemical formation of hydroxyl radical by constituents of natural waters. *Environ. Sci. Technol.* **1998**, *32*, 2947–2953.
- (6) Zhang, Y.; Del Vecchio, R.; Blough, N. V. Investigating the mechanism of hydrogen peroxide photoproduction by humic substances. *Environ. Sci. Technol.* **2012**, *46*, 11836–11843.
- (7) Canonica, S.; Freiburghaus, M. Electron-rich phenols for probing the photochemical reactivity of freshwaters. *Environ. Sci. Technol.* **2001**, *35*, 690–695.
- (8) Haag, W. R.; Hoigne, J.; Gassman, E.; Braun, A. M. Singlet oxygen in surface waters 0.1. Furfuryl alcohol as a trapping agent. *Chemosphere* **1984**, *13*, 631–640.
- (9) Haag, W. R.; Hoigne, J.; Gassman, E.; Braun, A. M. Singlet oxygen in surface waters 0.2. Quantum yields of its production by some natural humic materials as a function of wavelength. *Chemosphere* **1984**, *13*, 641–650.
- (10) Sharpless, C. M. Lifetimes of triplet dissolved natural organic matter (DOM) and the effect of NaBH_4 reduction on singlet oxygen quantum yields: Implications for DOM photophysics. *Environ. Sci. Technol.* **2012**, *46*, 4466–4473.
- (11) Zhou, X. L.; Mopper, K. Determination of photochemically produced hydroxyl radicals in seawater and fresh-water. *Mar. Chem.* **1990**, *30*, 71–88.
- (12) Gerecke, A. C.; Canonica, S.; Muller, S. R.; Scharer, M.; Schwarzenbach, R. P. Quantification of dissolved natural organic matter (DOM) mediated phototransformation of phenylurea herbicides in lakes. *Environ. Sci. Technol.* **2001**, *35*, 3915–3923.
- (13) Boreen, A. L.; Edlund, B. L.; Cotner, J. B.; McNeill, K. Indirect photodegradation of dissolved free amino acids: The contribution of singlet oxygen and the differential reactivity of DOM from various sources. *Environ. Sci. Technol.* **2008**, *42*, 5492–5498.
- (14) Bolton, J. R.; Linden, K. G. Standardization of methods for fluence (UV dose) determination in bench-scale UV experiments. *J. Environ. Eng.-ASCE* **2003**, *129*, 209–215.
- (15) Klassen, N. V.; Marchington, D.; McGowan, H. C. E. H_2O_2 determination by the I_3^- method and by KMnO_4 titration. *Anal. Chem.* **1994**, *66*, 2921–2925.
- (16) Sharpless, C. M.; Linden, K. G. Experimental and model comparisons of low- and medium-pressure Hg lamps for the direct and H_2O_2 assisted UV photodegradation of N-nitrosodimethylamine in simulated drinking water. *Environ. Sci. Technol.* **2003**, *37*, 1933–1940.
- (17) An, T. C.; Yang, H.; Li, G. Y.; Song, W. H.; Cooper, W. J.; Nie, X. P. Kinetics and mechanism of advanced oxidation processes (AOPs) in degradation of ciprofloxacin in water. *Appl. Catal. B-Environ.* **2010**, *94*, 288–294.
- (18) Haag, W. R.; Hoigne, J. Singlet oxygen in surface waters 0.3. Photochemical formation and steady-state concentrations in various types of waters. *Environ. Sci. Technol.* **1986**, *20*, 341–348.
- (19) Halladj, S.; Ter Halle, A.; Aguer, J. P.; Boulkamh, A.; Richard, C. Inhibition of humic substances mediated photooxygenation of furfuryl alcohol by 2,4,6-trimethylphenol. Evidence for reactivity of the phenol with humic triplet excited states. *Environ. Sci. Technol.* **2007**, *41*, 6066–6073.
- (20) al Housari, F.; Vione, D.; Chiron, S.; Barbati, S. Reactive photoinduced species in estuarine waters. Characterization of hydroxyl radical, singlet oxygen and dissolved organic matter triplet state in natural oxidation processes. *Photochem. Photobiol. Sci.* **2010**, *9*, 78–86.
- (21) Maddigapu, P. R.; Bedini, A.; Minero, C.; Maurino, V.; Vione, D.; Brigante, M.; Mailhot, G.; Sarakha, M. The pH-dependent photochemistry of anthraquinone-2-sulfonate. *Photochem. Photobiol. Sci.* **2010**, *9*, 323–330.
- (22) Burns, J. M.; Cooper, W. J.; Ferry, J. L.; King, D. W.; DiMento, B. P.; McNeill, K.; Miller, C. J.; Miller, W. L.; Peake, B. M.; Rusak, S. A.; Rose, A. L.; Waite, T. D. Methods for reactive oxygen species (ROS) detection in aqueous environments. *Aquat. Sci.* **2012**, *74*, 683–734.
- (23) Sun, L. Z.; Bolton, J. R. Determination of the quantum yield for the photochemical generation of hydroxyl radicals in TiO_2 suspensions. *J. Phys. Chem.* **1996**, *100*, 4127–4134.
- (24) Rosenfeldt, E. J.; Linden, K. G.; Canonica, S.; von Gunten, U. Comparison of the efficiency of OH radical formation during ozonation and the advanced oxidation processes $\text{O}_3/\text{H}_2\text{O}_2$ and UV/ H_2O_2 . *Water Res.* **2006**, *40*, 3695–3704.
- (25) Page, S. E.; Arnold, W. A.; McNeill, K. Terephthalate as a probe for photochemically generated hydroxyl radical. *J. Environ. Monit.* **2010**, *12*, 1658–1665.
- (26) Buxton, G. V.; Greenstock, C. L.; Helman, W. P.; Ross, A. B. Critical review of rate constants for reactions of hydrated electrons, hydrogen-atoms and hydroxyl radicals (OH/O^-) in aqueous-solution. *J. Phys. Chem. Ref. Data* **1988**, *17*, 513–886.
- (27) Canonica, S.; Jans, U.; Stemmler, K.; Hoigne, J. Transformation kinetics of phenols in water- photosensitization by dissolved natural organic material nad aromatic ketons. *Environ. Sci. Technol.* **1995**, *29*, 1822–1831.
- (28) Tratnyek, P. G.; Hoigne, J. Photooxidation of 2,4,6-trimethylphenol in aqueous laboratory solutions and natural waters—Kinetics of reaction with singlet oxygen. *J. Photochem. Photobiol. A-Chem.* **1994**, *84*, 153–160.
- (29) Golanoski, K. S.; Fang, S.; Del Vecchio, R.; Blough, N. V. Investigating the mechanism of phenol photooxidation by humic substances. *Environ. Sci. Technol.* **2012**, *46*, 3912–3920.
- (30) Maurino, V.; Borghesi, D.; Vione, D.; Minero, C. Transformation of phenolic compounds upon UVA irradiation of anthraquinone-2-sulfonate. *Photochem. Photobiol. Sci.* **2008**, *7*, 321–327.
- (31) Ononye, A. I.; McIntosh, A. R.; Bolton, J. R. Mechanism of the photochemistry of *p*-benzoquinone in aqueous-solutions 0.1. Spin trapping and flash-photolysis electron-paramagnetic resonance studies. *J. Phys. Chem.* **1986**, *90*, 6266–6270.
- (32) Page, S. E.; Arnold, W. A.; McNeill, K. Assessing the contribution of free hydroxyl radical in organic matter-sensitized photohydroxylation reactions. *Environ. Sci. Technol.* **2011**, *45*, 2818–2825.
- (33) Andreozzi, R.; Caprio, V.; Insola, A.; Marotta, R. Advanced oxidation processes (AOP) for water purification and recovery. *Catal. Today* **1999**, *53*, 51–59.
- (34) Aguer, J. P.; Richard, C. Photochemical behavior of a humic-acid synthesized from phenol. *J. Photochem. Photobiol. A-Chem.* **1994**, *84*, 69–73.
- (35) Chen, Y.; Hu, C.; Hu, X. X.; Qu, J. H. Indirect photodegradation of amine drugs in aqueous solution under simulated sunlight. *Environ. Sci. Technol.* **2009**, *43*, 2760–2765.
- (36) EPA. EPA Ultraviolet disinfection guidance manual for the final long term to enhanced surface water treatment rule, 2006.
- (37) Dong, M. M.; Rosario-Ortiz, F. L. Photochemical formation of hydroxyl radical from effluent organic matter. *Environ. Sci. Technol.* **2012**, *46*, 3788–3794.
- (38) Scully, F. E.; Hoigne, J. Rate constants for reactions of singlet oxygen with phenols and other compounds in water. *Chemosphere* **1987**, *16*, 681–694.
- (39) Wols, B. A.; Hofman-Caris, C. H. M. Review of photochemical reaction constants of organic micropollutants required for UV advanced oxidation processes in water. *Water Res.* **2012**, *46*, 2815–2827.

(40) Keen, O. S.; Love, N. G.; Linden, K. G. The role of effluent nitrate in trace organic chemical oxidation during UV disinfection. *Water Res.* **2012**, *46*, 5224–5234.

(41) Sharpless, C. M.; Seibold, D. A.; Linden, K. G. Nitrate photosensitized degradation of atrazine during UV water treatment. *Aquat. Sci.* **2003**, *65*, 359–366.

(42) Mostafa, S.; Rosario-Ortiz, F. L. Singlet oxygen formation from wastewater organic matter. *Environ. Sci. Technol.* **2013**, *47*, 8179–8186.